Sains Malaysiana 53(12)(2024): 3319-3328
http://doi.org/10.17576/jsm-2024-5312-15

Characterization of Graphene Oxide Functionalized Carbon Foam as a Potential Material for Different Applications

(Pencirian Span Melamin Berfungsian Grafin Oksida sebagai Elektrod Bahan Berpotensi bagi Aplikasi Pelbagai)

BALARABE EL-YAQUB[1,2], MOHD HANIFF WAHID[1,*], ZULKARNAIN ZAINAL[1,4], ABDUL HALIM ABDULLAH[1] & WAN AZLINA WAN AB KARIM GHANI[3]

[1]Department of Chemistry, Faculty of Science, Universiti Putra Malaysia, 43400 UPM Serdang, Selangor, Malaysia
[2]Department of Chemistry, Faculty of Science, Nigerian Defence Academy, Kaduna State, Nigeria
[3]Department of Chemical and Environmental Engineering, Faculty of Engineering, Universiti Putra Malaysia, 43400 UPM Serdang, Selangor, Malaysia
[4]Nanomaterials Synthesis and Characterizations Laboratory, Institute of Nanoscience and Nanotechnology, Universiti Putra Malaysia, 43400 UPM Serdang, Selangor, Malaysia

Received: 4 May 2024/Accepted: 18 October 2024

ABSTRACT

Due to its cheap production, high electrical conductivity, simplicity of doping, and enhanced hydrophilic characteristic, porous carbon foam has a lot of potential for energy storage and conversion applications. In this study, graphene oxide (GO) was successfully grafted onto carbon foam using a simple dip coating technique with the help of a linker. 3D porous carbon foams were created using a one-step carbonization from commercial melamine foam. The material was characterized using XRD, FTIR, BET, TGA, XPS, Raman and FESEM to confirm its structural, functional group, surface area, thermal stability, and morphological characteristics. The stress-strain tests of the samples were conducted on an electronic universal testing machine. These foams have sufficient surface area (99 m^2/g), a high level of C content (79.15%), and excellent compressibility. Moreover, as a proposed material for different applications, this distinctive GO grafted porous carbon foam also has the tendency to deliver remarkable performance in different fields of study. In conclusion, the GO grafted porous carbon foams have excellent prospects for different applications due to the straightforward preparation process and fascinating properties.

Keywords: Energy storage; graphene oxide; melamine foam; porous carbon foam

ABSTRAK

Foam karbon berliang memiliki potensi besar dalam aplikasi penyimpanan dan penukaran tenaga disebabkan oleh penghasilan yang murah, kekonduksian elektrik yang tinggi, proses pendopan yang mudah dan sifat hidrofilik yang unggul. Dalam kajian ini, grafin oksida telah berjaya dicantumkan pada foam karbon menggunakan teknik celupan mudah dengan kehadiran linker. Foam karbon berliang telah dihasilkan menggunakan satu langkah pengkarbonan dan proses aktivasi ke atas foam melamin komersial. Bahan telah dicirikan menggunakan XRD, FTIR, BET, XPS, Raman dan FESEM bagi mengesahkan struktur, kumpulan berfungsi, luas permukaan dan ciri morfologi. Ujian mampat dan regang ke atas sampel telah dijalankan dengan menggunakan ujian mesin universal elektronik. Foam ini memiliki luas permukaan yang tinggi (99 m^2/g), kandungan karbon yang tinggi (79.15%) dan kebolehmampatan cemerlang. Tambahan pula, sebagai elektrod cadangan bagi semua superkapasitor keadaan pepejal, foam karbon berliang istimewa ini memiliki kecenderungan untuk memberi kapasitan khusus yang mengagumkan. Secara kesimpulannya, foam karbon berliang memiliki prospek cemerlang bagi aplikasi pelbagai kerana proses penyediaan yang mudah dan sifat-sifat yang menakjubkan.

Kata kunci: Foam karbon; foam melamin; grafin oksida; penyimpanan tenaga; superkapasitor

INTRODUCTION

Porous carbon foams (PCF) synthesized from melamine sponge has been applied in a tremendous amount of fields recently for their various pore structures and larger specific surface area compared to other materials in fields of energy storage (Priya, Kennedy & Anand 2023; Wang & Hu 2018), adsorption (Shayesteh et al. 2023; Vorokhta et al. 2023), hydrogen storage (Asasian-Kolur et al. 2024; Muhammad et al. 2023) and oxygen reduction reaction (ORR) (Liu et al. 2023; Luo et al. 2023). They can be synthesized with low pollution and well controlled in pore size and channel. Particularly, they have high use period in cycle, chemical

inertness in interface, strong mechanical strength and good compressibility in structure and good performance in electrical conductivity.

Wearable electronic appliances are increasingly using flexible supercapacitors, which can maintain a stable power output while mechanically deformed (Delbari et al. 2021; Jiang & Lu 2021; Wang, Yang & Gao 2021). There have been numerous reports on the use of two-dimensional elastic supercapacitors as storage devices for energy for the creation of long-lasting, low-cost, and wearable electronic appliances (Chen et al. 2022; Muzaffar et al. 2023; Ponraj et al. 2021). Even though compression is a typical mechanical deformation encountered by wearable energy storage devices, compressible supercapacitors with 3D structures have received relatively little attention in research (Cao et al. 2022; Das et al. 2022). Studies have reported that compressible supercapacitors can be categorized into two. (1) Carbon materials that can support themselves as well as composites made of these carbon materials and conductive polymers, metal oxides, or hydroxides. The majority of these electrode materials exhibit excellent rate performance and cycling stability due to the superior electronic conductivity of carbon foams but rapid collapse of electrodes is caused by high stress, which is easy to destroy the structure of carbon foams. (2) Substrates that can be compressed and are packed with active ingredients, like cellulose aerogel and polymeric foam (Jain et al. 2023; Xu et al. 2020). Polymeric foams as substrates have exceptional compressive properties, but substrates that are insulative have a limit on the rate capability and capacitance of these electrodes. As a result, creating a compressible supercapacitor with excellent electrochemical performance and high compressibility is highly desirable. Due to its excellent durability, water absorption, and compressibility, the melamine foam (MS) with a porous three-dimensional (3D) network is frequently used as a compressible substrate.

Another field of research that these materials can be applied is adsorption. Several studies have reported the use of porous carbon foams for adsorption of different materials (Vorokhta et al. 2023) investigated the contribution of introducing nitrogen to the porous structure and the CO_2 intake capacity of the hierarchically porous carbon foam (PCF) at different synthesis condition (pressure and temperature). Different content of nitrogen (7-13%) was synthesized by reacting C_2H_5ONa with different amounts of amino alcohols (namely mono, di and triethanolamine) after which heat was introduced to decompose the product. The physico-chemical properties were investigated using suitable techniques. The product of this reaction comprised different porous structure which included micro and mesopores all around the carbon walls. It was found from the results that the foam with the least amount of nitrogen (7%) and volumetric porosity of 0.44 cm^3/g and surface area of 1549 m^2/g showing the highest CO_2 adsorption, up-taking 5.14 mmol/g at absolute temperature, 3.22 mmol/g at 298 K and 1.93 mmol/g at 323 K. The doped PCF adsorbed more CO_2 better than the undoped foam, despite showing an inferior physico-chemical properties. This study shows the significance of nitrogen species in CO_2 adsorption, but also shows that by increasing the nitrogen content, this leads to the lowering of the micropore volume giving rise to poor CO_2 adsorption. Superior N_2/CO_2 selectivity with excellent separation of CO_2 from N_2-CO_2 gaseous mixture, quick uptake through physical adsorption and high cycling stability were also noticed indicating that these materials have high regenerability.

Another study by Rong et al. (2023) fabricated a three-dimensional (3D) porous carbon material which showed a promising characteristics as a potential adsorbent because of its outstanding benefits such as improved porosity and surface area. However, not much research has been done to increase the performance by tuning the microstructures. The authors reported in this work how metallic nanoparticles were encapsulated on carbonized melamine foam functionalized with carbon nanotubes using a straight forward chemical and pyrolytic procedure. The microstructural and adsorption characteristics through microwave technique were studied alongside dielectric/magnetic deficiencies were also investigated. During the pyrolytic process, the metallic nanoparticles were encapsulated on the 3D porous foam via *in-situ* growth. The carbon nanotubes and the metallic constituents' structure could be monitored by regulating the concentration of the precursor thereby tuning the absorption activity of the material. The CNTs/CF-3:0 composite is attributed to numerous interface reflections, dielectric/magnetic deficiencies, variable polarization behavior, and enhanced impedance matching. These factors allow for an ultra-wide responsive bandwidth (4.1–18.0 GHz with RL value exceeding − 10 dB) and significant reflection loss (− 75.4 dB at 5.2 GHz). A 3D network framework of this kind acknowledges its reduced density. The intricate design and synthesis of submicron-scale structures of three-dimensional porous carbon-based absorbent materials was sparked by these results, which also served as inspiration (Rong et al. 2023).

Shayesteh et al. (2023) conducted a study on the development of two reusable foamy-based, ultrahydrophobic/ultraoleophilic eco-friendly adsorbents for the separation of oil and water mixtures. In order to develop a ultrahydrophobic/ultraoleophilic, reusable, and reusable three-dimensional porous structure, hierarchically biomass-derived porous carbon (PC) and multi-walled carbon nanotube (MWCNT) were first synthesized and loaded on pristine melamine foam (MF) using a straightforward dip-coating approach by combining silicone adhesive. The produced materials exhibited good micro-mesoporous frameworks and a large specific surface area of 240 m^2/g (MWCNT) and 1126 m^2/g (PC).

Additionally, these structures' exceptional capacity for recycling and reuse ability in ten adsorption-squeezing

cycles showed that, even after soaking in salty (3.5% NaCl) and acidic (pH=2) and alkaline (pH=12) solutions, the WCA and sorption capacity remained largely unchanged. More importantly, the superhydrophobic samples' chemical stability and reusability make them excellent candidates for use in a variety of challenging environments for oil spill cleaning.

Ma et al. (2023) additionally produced trimetallic (Fe, Co, Ni) spinel/carbon/nickel foam (FeCoNiOx/C/NF) electrodes with 3D network configurations, and shown that oxygen bubbles can be swiftly be expelled from the surface of electrodes with ultrahydrophilic/ultraaerophobic qualities. At a current density of 10 $mAcm^{-2}$ in 1 M KOH, the resulting FeCoNiOx/C/NF electrodes showed an extraordinarily low Tafel slope of 21 $mVdec^{-1}$, along with a low over-potential of 221 mV. FeCoNiOx/C/NF electrodes demonstrated a low over-potential of 325 mV with long-term stability for 250 h at a high current density of 500 $mAcm^{-2}$.

Herein, a complex 3D self-supported carbonaceous structure combined with thermally reduced graphene oxide was synthesized by using a simple dip coating method. Through the decomposition of melamine foam through pyrolysis, carbon foam-doped rGO with a dimension of 3 cm × 1 cm × 1 cm was prepared. The combination of rGO with the porous material will not only ensure high performance but also can greatly improve the cycling stability and recyclability of the material. In particular, the outer rGO sheets were introduced to form a continuous conductive network, which improves the electronic conductivity of the material. Meanwhile, the elasticity of the porous material makes the structure of the electrodes firm enough to avoid collapsing under a high compressive strain.

EXPERIMENTAL DETAILS

PREPARATION OF GO

Graphene oxide was prepared using a modified Hummers process (Marcano et al. 2010), few grams of graphite was dispersed in a 9 : 1 acid mixture (200 mL) of concentrated H_2SO_4/H_3PO_4. After this, 9.0 g of $KMnO_4$ was gently added to the mixture and stirred for 3 days. 35 mL of H_2O_2 was then added carefully to the mixture, which was stirred for a day at room temperature to completely oxidize the excess $KMnO_4$ and terminate the oxidation process. The graphene oxide was then washed and centrifuged with 1M HCl and excess DI water.

FABRICATION OF 3D POROUS CARBON FOAM

A commercialized melamine sponge with dimension (1 cm^3) was carbonized for two hours at 400 °C in a tube furnace with a N_2 environment. Ethanol and deionized water were used to clean the resultant materials. The foam was activated in an alkaline medium by increasing the alkaline/carbon weight ratios to 1:4 and immersing it in deionized water after it had dried at 80 °C for an entire night. Overnight, the mixes were dried at 80 °C. Following a diluted HCl solution (5%) wash, the resultant porous materials were dried. Ultimately, PCF– 1:4 was assigned to the activated samples.

PREPARATION OF POROUS CARBON FOAM-GO (PCF/GO)

The synthesis process of PCF/GO composite is illustrated in Figure 1. Firstly, ethanol, epichlohydrin and NaOH (1 M) were added together in the ratio of 13:1:0.1 to produce a linker solution. Then, the carbon foam was dipped in the linker solution for 2 min and then squeezed and allowed to dry for about 30 min in a fume hood. The resulting PCF was then dipped in 2 mg/mL solution of GO for 2 min and transferred to an oven for drying at 100 °C for 24 h. The as-prepared dried composite was denoted as PCF/GO composite.

CHARACTERIZATION

The structure and morphology of the doped porous carbon materials were extensively characterized using different techniques such as field emission scanning electron microscopy (FESEM; Hitachi SU-8000) attached with energy dispersive X-ray spectroscopy (EDX), Brunauer-Emmett-Teller (BET) surface area analysis, Fourier transform infrared (FTIR; IFS-85) spectrometer, X-ray diffraction (XRD), Raman spectroscopy and compressive strength test.

ELEMENTAL ANALYSIS

Elemental analyses of porous carbon-based materials were determined using an energy dispersive X-ray analyzer (FEI-Quanta 200) directly linked to a field emission scanning electron microscopy (FESEM; Hitachi SU-8000).

X-RAY DIFFRACTION

XRD is a non-destructive technique for qualitative analysis. XRD was used to compare the XRD pattern of porous carbon materials. The analysis was conducted from 4° to 90° by using a 2θ goniometer X-ray powder diffractometer (PANalytical X'pert-Pro MPD PW 3040), operated at Cu-K α radiation (λ = 0, 15406 nm). The diffractogram was scanned at a scan rate of 2° min^{-1}.

THERMOGRAVIMETRIC ANALYSIS

Thermogravimetric analysis (TGA) was used to study the thermal decomposition of porous carbon materials by using Metter-Toledo thermogravimetric analyzer. The materials with particle size ≤45 μm was placed in a 40 μL alumina crucible and subjected to heating in the range of 25 °C to 1000 °C at 10 °C/min under the flow of nitrogen gas at 50 mL/min.

FOURIER TRANSFORM INFRARED SPECTROSCOPY

Fourier Transform Infrared (FTIR) spectroscopy was used to analyze the functional groups of the nitrogen-rich porous carbon materials. A Perkin- Elmer FTIR spectrometer coupled with UATR accessory was used to record FTIR transmittance spectra. Approximately 0.001 g of sample was used and scanned within the wavenumber of 400 cm^{-1} to 4000 cm^{-1}.

FIELD EMISSION SCANNING ELECTRON MICROSCOPY

The morphology of the carbon materials was studied using a field emission scanning electron microscopy (FE-SEM, Hitachi SU-8000).

BRUNAUER-EMMETT-TELLER (BET) SURFACE AREA ANALYSIS

N_2 adsorption-desorption isotherms were determined on a Micrometrics ASAP 2020 instrument at 77 K. The specific surface area and pore size distribution were carried out by the Brunauer– Emmett–Teller (BET) method.

X-RAY PHOTOELECTRON SPECTROSCOPY (XPS)

The surface chemical compositions of the samples were investigated using axis ultra (kratos analytical ltd) with monochromatic Mg Kα radiation (1253.6 eV) as the excitation source. The peak fitting and deconvolution were performed using the origin 2024 software package. The baseline of spectra was subtracted (Shirley type), and all peaks were assumed to be Gaussian type. The calibration of binding energy of the spectra was referenced to the C_{1s} electron bond energy corresponding to graphitic carbon at 284.6 eV to compensate for surface charging effects.

COMPRESSIVE STRENGTH TEST

Mechanical characteristics of the porous carbon materials were tested during the compressing and recovering process. The stress-strain tests of the samples were conducted on an electronic universal testing machine (Instron8874).

RESULTS AND DISCUSSION

Preparation of carbon foams as illustrated in Figure 1(b) can serve as monumental supercapacitor electrodes to carry out electrochemical characterization. Melamine foam not only provides low density and high porosity, providing enough spaces to accommodate activating agent. After undergoing pyrolytic process at 600 °C and activation treatment, it was found that the obtained carbon foam showed a significant reduction in volume and color change from white to black (Figure 3(b)). The morphology of the foams were investigated using FESEM. The activation process through the use of KOH induced numerous micro-sized holes on the skeleton of the carbon foam. It should be noted that through activation using KOH treatment, not only enhanced the contact area between the electrode and the electrolyte but also facilitate electrolyte ion diffusion, which are favorable for high specific capacitance and improved performance (Jing et al. 2021).

ENERGY DISPERSIVE X-RAY ANALYSIS

Table 1 shows the weight percentage of the composition of melamine, carbon foam and GO grafted carbon foam. It was found that the major component of melamine was nitrogen with the presence of some amount of carbon which is another constituent of the melamine foam (Yan et al. 2022). After pyrolysis of the melamine foam, the amount of carbon increased which shows the conversion of the melamine foam to carbon foam. Upon grafting of GO on the carbon foam with the use of linker, the amount of carbon decreased because of the introduction of oxygen from the graphene oxide. The percentage of oxygen in the GO carbon foam shows a successful grafting of GO into the carbon foam. The presence of other elements like Na and Cl might be attributed to the linker used in holding the GO to the carbon foam.

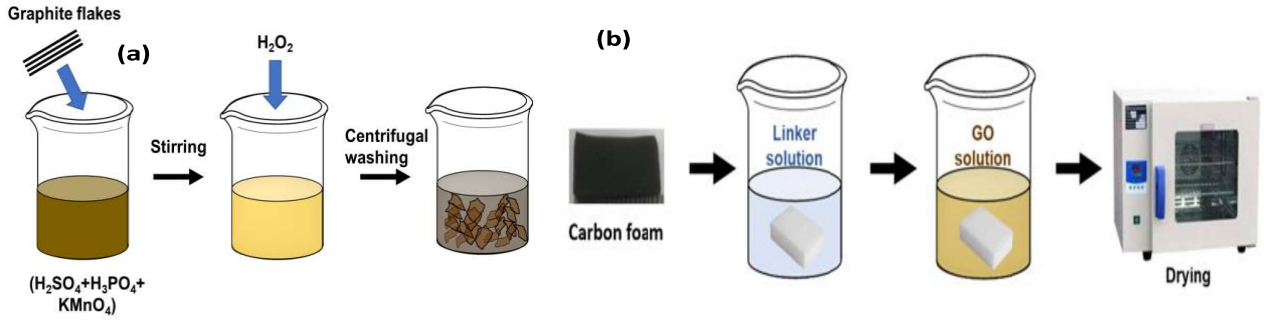

FIGURE 1. (a) Schematic illustration of the synthesis of graphene oxide (b) Schematic illustration of the synthesis process of porous carbon foam-GO materials

X-RAY DIFFRACTION

Figure 2 shows the XRD results of pure melamine, carbon foams, activated carbon foams and GO grafted carbon foams. The results showed successful transformation of melamine foam to carbon foam with the appearance of a prominent peak at 72.66° with miller indices (0 2 3) with reference stick pattern of ICSD card no. 98-002-8292. This peak can be attributed to the increase in the amount of carbon in the foam as seen in other foams of the carbon foam. Upon grafting the carbon foam with GO an additional weak peak at around 10.20° was seen which can be attributed to GO as reported in several literatures (Shen et al. 2019; Zhu et al. 2023).

THERMOGRAVIMETRIC ANALYSIS

The TGA measurement was done to ascertain the thermal stability of the porous materials as shown in Figure 3. For the melamine foam, there was rapid decomposition of the foam as the temperature raised from 0 °C to around 700 °C. This shows that there was no formation of any stable intermediate as the temperature rises. For the porous carbon foams, there was a formation of a stable intermediate at a temperature a little bit above 200 °C which can be attributed to dehydration or loss of volatile constituents in the porous foam. When rGO was grafted on the porous foam, a reasonable amount of thermal stability was achieved showing there was no decomposition of the

TABLE 1. The weight percentage of melamine, carbon foam and GO-carbon foam

Sample	C(%)	N(%)	O(%)
Melamine	38.82	59.76	-
Carbon foam	79.15	-	12.32
GO-carbon foam	69.86	-	26.07

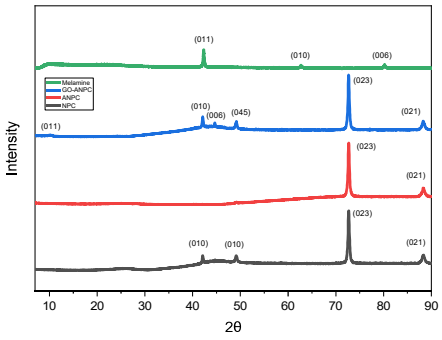

FIGURE 2. XRD pattern for melamine foam, carbon foam, activated carbon foam and GO grafted carbon foam

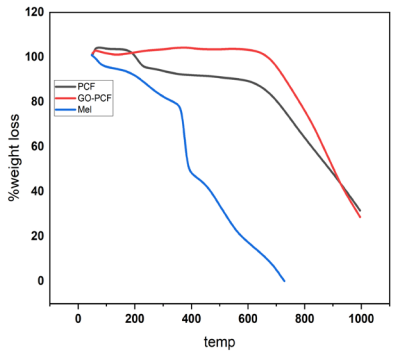

FIGURE 3. TGA thermogram of melamine, porous carbon foam and GO-porous carbon foam

material even when the temperature was risen to almost 800 °C. This shows that the introduction of rGO to the porous carbon foams increases the thermal stability of the materials.

FTIR SPECTROSCOPY ANALYSIS

The FTIR spectra of the samples are as shown in Figure 4. As can be observed, melamine foam exhibits characteristics peaks at 1531 cm^{-1}, 1162 cm^{-1}, and 995 cm^{-1} which can be attributed to triazine ring structure, C-N of amino and C-O of methylol (Xu et al. 2020). In addition to this, another characteristic peak at 3370 cm^{-1} is seen and can be attributed to the superposition of stretching vibrations of O-H (hydroxyl group) and N-H (amino group). In the FTIR spectrum of porous carbon foam, the peaks around 1271 cm^{-1} can be attributed to C-C bond while other peaks around 833 cm^{-1} and 785 cm^{-1} corresponds to C-O bonds. The disappearance of the C-N peak at 3370 cm^{-1} shows the formation of the porous carbon foam which has carbon as the major constituent as showed by the EDX results in Table 1. After grafting of rGO on the porous carbon foam, several peaks which can be attributed the rGO appeared. These peaks include 1650 cm^{-1}, 1540 cm^{-1}, 1457 cm^{-1}, and 1395 cm^{-1} corresponding to C=C bond and C=O bonds of alkenes and carbonyl groups, respectively. Weak peaks at 2360 cm^{-1} and 2339 cm^{-1} were also noticed showing that rGO have been successfully grafted on the porous carbon as seen in the images from FESEM in Figure 5.

FESEM

Surface morphology of melamine, carbon foam and GO-carbon foam are as shown in Figure 5(c), 5(d) and 5(f). All images exhibit three dimensional porous structure. The three-dimensional (3D) interconnected porous structure of melamine shows fine large uniform pores (Figure 5(c)). After pyrolysis, the as-prepared carbon foam still inherits the porous structure but with additional pores (Figure 5(d), 5(e)). Furthermore, there is ~60% volume shrink of carbon foam (Figure 5(b)) compared to that of melamine foam (Figure 5(a)) observed

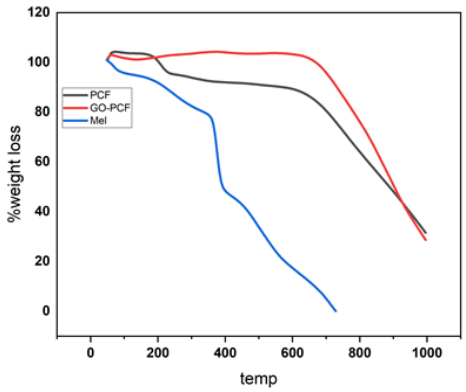

FIGURE 4: TGA thermogram of melamine, porous carbon foam and GO-porous carbon foam

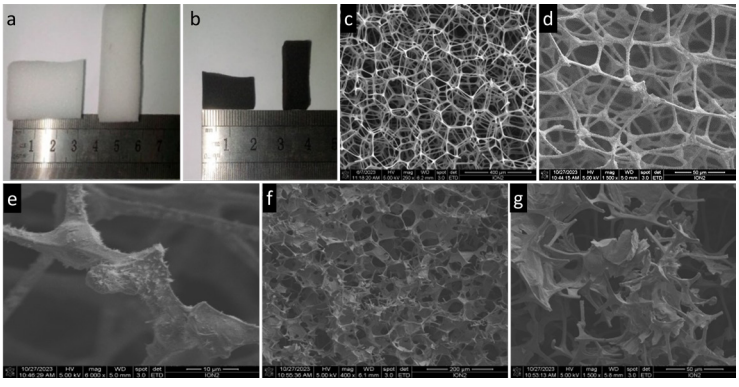

FIGURE 5. Development of PCF and PCF-GO. Photograph images of melamine foam (a) and carbon foam (b). SEM images of melamine foam (c), carbon foam (d,e) and GO carbon foams (f,g)

The FESEM images of carbon foams hybrids in which GO are encapsulated in the open edges of 3D porous structure containing carbon atoms acted as spacers to keep the neighboring graphene oxide sheets attached to the foam as seen in Figure 5(f) and 5(g). The FESEM images of GO-carbon foam illustrated that surface and inner structure of the foam was covered by GO NSs (Figure 5(f), 5(g)), which can influence the mechanical properties of the foam and provide additional active sites for electron accumulation.

RAMAN SPECTROSCOPY

The Raman spectrum of porous carbon foam exhibits two intensive peaks of 1564 cm^{-1} and 1355 cm^{-1} corresponding to D and G bands (Kumar et al. 2020). GO grafted porous carbon foam also exhibited peaks at 1560 cm^{-1} and 1347 cm^{-1} also corresponding to the G and D band, respectively. The D band comes from the lattice structure defects whereas the G band is related to the well documented graphitic band. The peak intensity ratio (I_D and I_G) values of the materials are 0.87 and 0.86 corresponding to porous carbon foams and GO grafted porous foams which shows that the structural order or defects degree of carbonaceous materials is very high (Jing et al. 2021) (Figure 6).

BET

To ascertain the porosity of the doped porous carbon foams and porous carbon foams, the N_2 adsorption-desorption analysis was carried out. The porous carbon foams displayed an isotherm of the typical mesoporous kind. Enhancing the materials' rate performance is the mesopore's basic purpose.

In order to examine the structural alterations of the porous carbon foams, Table 2 provides the corresponding porous structure parameters that were computed using the N_2 adsorption-desorption isotherms. The specific surface area decreased based on the concentration of rGO deposited on the porous foam, from 99 m^2/g to 44.18 m^2/g. This shows that the rGO components have been effectively loaded onto the porous foams, reducing the surface area by filling the material's pores.

In addition to improving the activity and performance, the accessible surface area, appropriate pore size distribution, and well-developed nanostructure are advantageous for electrolyte penetration, adsorbent diffusion and quick ions diffusion among others. The ability of the porous materials to accommodate dopants like rGO can also help increase the performance of the materials as solid electrodes for supercapacitors since these dopants have high conductive properties.

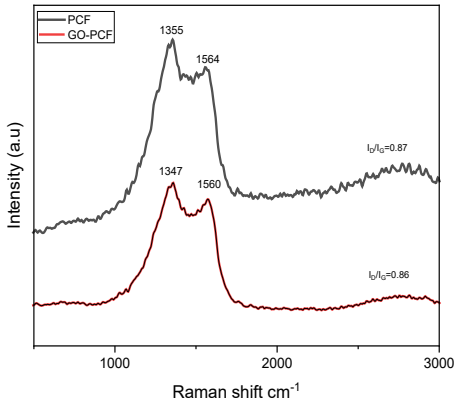

FIGURE 6. Raman spectroscopy for porous carbon forms and GO coated porous carbon foam

TABLE 2. Characteristics of the porous structure determined from the nitrogen adsorption-desorption isotherms

Sample	S/area (m^2/g)	Pore volume (cm^3/g)	Pore size (nm)
PCF	99.00	0.5677	4.7862
0.02 PCF	90.97	0.4012	5.0261
0.04 PCF	62.28	0.4026	5.3064
0.06 PCF	56.67	0.4679	5.1204
0.08 PCF	44.18	0.5052	5.6592

X-RAY PHOTOELECTRON SPECTROSCOPY (XPS)

Figure 7 shows that the PCF-rGO-ppy material constitutes mainly O 1s, N 1s and C 1s signals. The surface atomic percentages by mass of C, O and N in the material are 77.71%, 16.19%, and 6.16%, respectively, as shown is the survey spectrum from Figure 7(a). The N spectra in Figure 7(b) demonstrated the presence of N=O at 397.61 eV, C–N at 399.83 eV, and N=O at 401.25 eV. This supports that rGO-PPy is successfully anchored on the PCF's surface, as seen by the N1s peak of PPy in Figure S2. The C1s spectrum in Figure 7(c) displays the coexistence of the C=C chemical state at 283.9 eV, C–C at 284.81 eV, C–N/C–O at 285.72 eV, and the C=N/C=O chemical state at 287.45 eV. According to Fang et al. (2020), the satellite peak of C1s is located at 290.59 eV and represents molecular structural information. It could represent the benzene ring's pi-pi* transition. This is in line with the rGO and PPy C1s peak data as shown in Figures S1 and S2, respectively.

COMPRESSIVE STRENGTH TEST

To assess the compressibility of the porous carbon foam, compression experiments were performed at a rate of 1.2 cm^{-1}. The functionalized porous carbon foams can fully regain their original shape without deformation at various compressive stresses (0%, 30%, 50%, and 80%) when the strains are released (Figure 8). Figure 8(b) displays the functionalized porous carbon's stress-strain curves at various compression strains. The stresses that the porous carbon foams can tolerate at 30%, 50%, and 80% strains, respectively, are 12.70, 17.90, and 28.89 KPa.

The results displayed in Figure 8(c) show how the mechanical properties were further assessed by repeated compression and release procedure for 200 cycles at a constant strain of 80%. The robust structure and good elasticity of the porous carbon foam further confirmed by the stress-strain curve's ability to keep its shape after 200 cycles of the compression test, exhibiting a notable hysteresis loop.

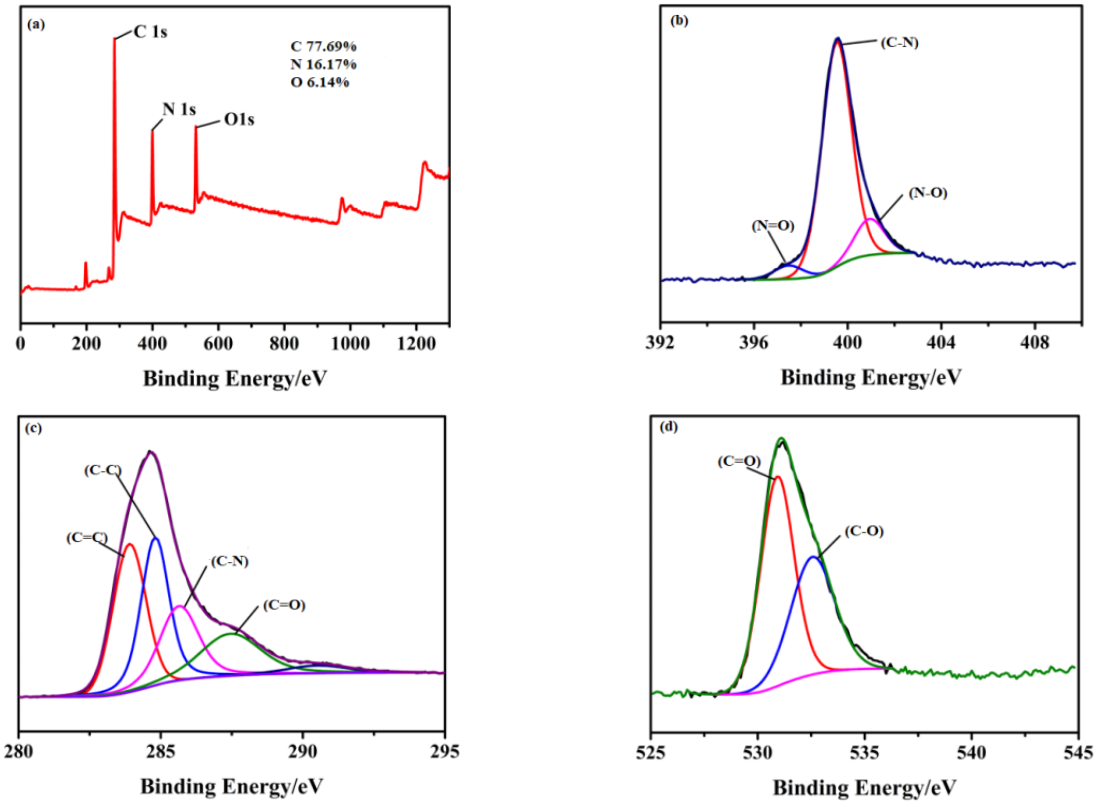

FIGURE 7. Full XPS spectrum of PCF-rGO-ppy (a); survey spectrum (b) High-resolution XPS spectra of N 1s (c), C 1s (d) and O1s

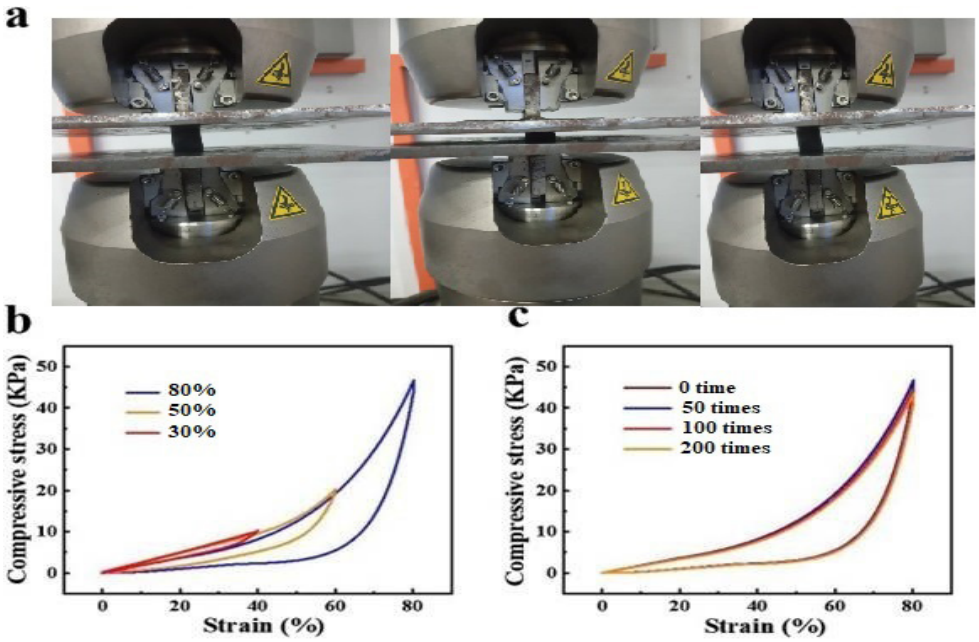

FIGURE 8. (a) Photographs of PCF-rGO-ppy during the compression and recovery process, (b) The stress-strain curves of PCF-rGO-ppy under different compressive strain, (c) The stress–strain curves after different compressing-recovering cycles

CONCLUSION

In summary, graphene oxide was successfully grafted on carbon foam by simple dip coating technique. Due to its compressible structure, 3D structured carbon foams can be used as a flexible substrate because it can still maintain its initial shape after 200 cycles of compression test. The material was successfully characterized using XRD, FTIR, BET, TGA, XPS, Raman and FESEM to confirm its structural, functional groups, surface area, thermal stability and morphological properties. The material has a sufficient surface area and high level carbon content. From the results obtained material showed exceptional properties which can be used for different applications.

ACKNOWLEDGEMENTS

This work has been supported by Universiti Putra Malaysia, through grant no: Geran Putra GP-IPS/2023/9746900. The authors declare that they do not have any conflicts of interest.

REFERENCES

Asasian-Kolur, N., Sharifian, S., Haddadi, B., Jordan, C. & Harasek, M. 2024. Ordered porous carbon preparation by hard templating approach for hydrogen adsorption application. *Biomass Conversion and Biorefinery* 14(16): 18381-18416.

Cao, W., Ling, S., Chen, H., He, H., Li, X. & Zhang, C. 2022. 3D-printed ultralight, superelastic reduced graphene oxide/manganese dioxide foam for high-performance compressible supercapacitors. *Industrial & Engineering Chemistry Research* 61(30): 10922-10930.

Chen, X., Yu, H., Gao, Y., Wang, L. & Wang, G. 2022. The marriage of two-dimensional materials and phase change materials for energy storage, conversion and applications. *EnergyChem* 4(2): 100071.

Das, H.T., Dutta, S., Balaji, T.E., Das, N., Das, P., Dheer, N., Kanojia, R., Ahuja, P. & Ujjain, S.K. 2022. Recent trends in carbon nanotube electrodes for flexible supercapacitors: A review of smart energy storage device assembly and performance. *Chemosensors* 10(6): 223.

Delbari, S.A., Ghadimi, L.S., Hadi, R., Farhoudian, S., Nedaei, M., Babapoor, A., Namini, A.S., Van Le, Q., Shokouhimehr, M. & Asl, M.S. 2021. Transition metal oxide-based electrode materials for flexible supercapacitors: A review. *Journal of Alloys and Compounds* 857: 158281.

Fang, D., He, F., Xie, J. & Xue, L. 2020. Calibration of binding energy positions with C1s for XPS results. *Journal of Wuhan University of Technology-Mater. Sci. Ed.* 35(4): 711-718.

Jain, A., Ziai, Y., Bochenek, K., Manippady, S.R., Pierini, F. & Michalska, M. 2023. Utilization of compressible hydrogels as electrolyte materials for supercapacitor applications. *RSC Advances* 13(17): 11503-11512.

Jiang, L. & Lu, X. 2021. Functional hydrogel-based supercapacitors for wearable bioelectronic devices. *Materials Chemistry Frontiers* 5(20): 7479-7498.

Jing, X., Wang, L., Qu, K., Li, R., Kang, W., Li, H. & Xiong, S. 2021. KOH chemical-activated porous carbon sponges for monolithic supercapacitor electrodes. *ACS Applied Energy Materials* 4(7): 6768-6776. https://doi.org/10.1021/acsaem.1c00868

Kumar, R., Youssry, S.M., Soe, H.M., Abdel-Galeil, M.M., Kawamura, G. & Matsuda, A. 2020. Honeycomb-like open-edged reduced-graphene-oxide-enclosed transition metal oxides (NiO/Co_3O_4) as improved electrode materials for high-performance supercapacitor. *Journal of Energy Storage* 30: 101539. https://doi.org/10.1016/j.est.2020.101539

Liu, H., Jiang, L., Wang, Y., Wang, X., Khan, J., Zhu, Y., Xiao, J., Li, L. & Han, L. 2023. Boosting oxygen reduction with coexistence of single-atomic Fe and Cu sites decorated nitrogen-doped porous carbon. *Chemical Engineering Journal* 452: 138938.

Luo, Y., Wen, M., Zhou, J., Wu, Q., Wei, G. & Fu, Y. 2023. Highly-exposed Co-CoO Derived from nanosized ZIF-67 on N-doped porous carbon foam as efficient electrocatalyst for zinc-air battery. *Small* 19(43): 2302925.

Ma, L., Wei, Z., Zhao, C., Meng, X., Zhang, H., Song, M., Wang, Y., Li, B., Huang, X. & Xu, C. 2023. Hierarchical superhydrophilic/superaerophobic 3D porous trimetallic (Fe, Co, Ni) spinel/carbon/nickel foam for boosting oxygen evolution reaction. *Applied Catalysis B: Environmental* 332*:* 122717.

Marcano, D.C., Kosynkin, D.V., Berlin, J.M., Sinitskii, A., Sun, Z., Slesarev, A., Alemany, L.B., Lu, W. & Tour, J.M. 2010. سنتز اکسید گرافن بهبود یافته است. *ACS Nano* 4(8): 4806-4814. https://pubs.acs.org/doi/abs/10.1021/nn1006368

Muhammad, R., Park, J., Kim, H., So, S.H., Nah, Y-C. & Oh, H. 2023. Facile synthesis of ultrahigh-surface-area and hierarchically porous carbon for efficient capture and separation of CO_2 and enhanced CH_4 and H_2 storage applications. *Chemical Engineering Journal* 473: 145344.

Muzaffar, N., Afzal, A.M., Hegazy, H.H. & Iqbal, M.W. 2023. Recent advances in two-dimensional metal-organic frameworks as an exotic candidate for the evaluation of redox-active sites in energy storage devices. *Journal of Energy Storage* 64: 107142.

Ponraj, J.S., Narayanan, M.V., Dharman, R.K., Santiyagu, V., Gopal, R. & Gaspar, J. 2021. Recent advances and need of green synthesis in two-dimensional materials for energy conversion and storage applications. *Current Nanoscience* 17(4): 554-571.

Priya, D.S., Kennedy, L.J. & Anand, G.T. 2023. Emerging trends in biomass-derived porous carbon materials for energy storage application: A critical review. *Materials Today Sustainability* 2023: 100320.

Rong, H., Song, H., Gao, T., Li, Y., Zhao, R. & Zhang, X. 2023. Ultralight melamine foam derived metal nanoparticles encapsulated CNTs/porous carbon composite for electromagnetic absorption. *Synthetic Metals* 294: 117306.

Shayesteh, H., Khosrowshahi, M.S., Mashhadimoslem, H., Maleki, F., Rabbani, Y. & Emrooz, H.B.M. 2023. Durable superhydrophobic/superoleophilic melamine foam based on biomass-derived porous carbon and multi-walled carbon nanotube for oil/water separation. *Scientific Reports* 13(1): 4515.

Shen, T., Zhao, Z., Zhong, Q., Qin, Y., Zhang, P. & Guo, Z.X. 2019. Preparation of graphene/Au aerogel film through the hydrothermal process and application for H_2O_2 detection. *RSC Advances* 9(23): 13042-13047. https://doi.org/10.1039/c9ra00516a

Vorokhta, M., Kusdhany, M.I.M., Vörös, D., Nishihara, M., Sasaki, K. & Lyth, S.M. 2023. Microporous carbon foams: The effect of nitrogen-doping on CO_2 capture and separation via pressure swing adsorption. *Chemical Engineering Journal* 471: 144524.

Wang, L. & Hu, X. 2018. Recent advances in porous carbon materials for electrochemical energy storage. *Chemistry–An Asian Journal* 13(12): 1518-1529.

Wang, M., Yang, Y. & Gao, W. 2021. Laser-engraved graphene for flexible and wearable electronics. *Trends in Chemistry* 3(11): 969-981.

Xu, M., Ma, Y., Liu, R., Liu, Y., Bai, Y., Wang, X., Huang, Y. & Yuan, G. 2020. Melamine sponge modified by graphene/polypyrrole as highly compressible supercapacitor electrodes. *Synthetic Metals* 267(June): 1-9. https://doi.org/10.1016/j.synthmet.2020.116461

Yan, C., Luo, Y., Zhang, W., Zhu, Z., Li, P., Li, N., Chen, Y. & Jin, T. 2022. Preparation of a novel melamine foam structure and properties. *Journal of Applied Polymer Science* 139(16): 51992.

Zhu, X., Zhou, G., He, G., Ma, L., Xu, B. & Sun, F. 2023. Directly loading graphene oxide into melamine sponge for fast and high-efficiency adsorption of methylene blue. *Surfaces and Interfaces* 36: 102575. https://doi.org/10.1016/j.surfin.2022.102575

*Corresponding author; email: mw_haniff@upm.edu.my